## A simulator for quantum computer hardware

Michielsen, K.F L; de Raedt, Hans; De Raedt, K.

# A simulator for quantum computer hardware

**Kristel Michielsen[1], Hans De Raedt[1,3] and Koen De Raedt[2]**

[1] Institute for Theoretical Physics and Materials Science Centre, University of Groningen,
Nijenborgh 4, NL-9747 AG Groningen, The Netherlands
[2] European Marketing Support, Vlasakker 21, B-2160 Wommelgem, Belgium

E-mail: kristel@phys.rug.nl and deraedt@phys.rug.nl

**Abstract**
We present new examples of the use of the quantum computer (QC)
emulator. For educational purposes we describe the implementation of the
CNOT and Toffoli gate, two basic building blocks of a QC, on a three qubit
NMR-like QC.

## 1. Introduction

Quantum computers (QCs) have recently become of great interest, primarily due to their potential of solving certain computationally hard problems such as factoring integers [1] and searching databases faster than a conventional computer [2]. In principle there is nothing a QC can do that a conventional computer cannot do but quantum mechanics may allow us to calculate faster. The fact that a QC might be more powerful than an ordinary computer is based on the notion that a quantum system can be in a superposition of states and that this allows exponentially many computations to be done in parallel. In experiments, the operation of elementary quantum logic gates using ion traps, cavity QED, and NMR technology has been demonstrated. Primitive QCs have been built [3–6].

Just as simulation is an integral part of the design process of each new generation of microprocessors, software to emulate the physical model representing the hardware implementation of a quantum processor may prove essential. In contrast to conventional digital circuits where the internal working of each basic unit is irrelevant for the logical operation of the whole machine, in a QC the internal quantum dynamics of each elementary constituent is a key ingredient of the QC itself. Therefore, it is essential to incorporate into a simulation model the physics of the elementary units that make up the QC.

Theoretical work on quantum computation usually assumes the existence of units that perform highly idealized unitary operations. However, in practice these operations are difficult to realize: disregarding decoherence, a hardware implementation of a QC will perform unitary operations that are more complicated than those considered in most theoretical

work. Therefore it is important to have theoretical tools to validate designs of physically realizable quantum processors.

Recently, a quantum computer emulator (QCE) has been developed [9] to emulate various hardware designs of QCs. The QCE consists of a simulator of a generic, general purpose QC and a graphical user interface [9]. The simulator simulates the physical processes that govern the operation of the hardware quantum processor, strictly according to the laws of quantum mechanics. The graphical user interface is used to control the simulator, to define the physical realization of the QC and to debug and execute quantum algorithms (QAs). The QCE runs in a Windows 98/NT/2000 environment [9]. It can be used as a research tool to validate designs of physically realizable quantum processors and as an educational tool to learn about QCs and QAs in an interactive way.

In this paper we present new applications of the QCE. We focus on the educational aspects of the QCE. For pedagogical reasons we show how to implement the CNOT and Toffoli gate on QCs using ideal units and more realistic qubits, such as those used in NMR QCs [3–6]. Although the CNOT and Toffoli gate are basic building blocks of a QC, the implementation of the latter on various types of QCs is not, as far as we know, documented in the literature.

## 2. Quantum computer emulator

### 2.1. Simulator

QC hardware can be modelled in terms of quantum spins (qubits) that evolve in time according to the time-dependent Schrödinger equation (TDSE)

$$i\frac{\partial}{\partial t}|\Phi(t)\rangle = H(t)|\Phi(t)\rangle, \qquad (1)$$

---

[3] http://rugth30.phys.rug.nl/compphys

K Michielsen *et al*

in units such that $\hbar = 1$. For pedagogical reasons we will consider three qubit QCs only. The state

$$|\Phi(t)\rangle = a(\downarrow,\downarrow,\downarrow;t)|\downarrow,\downarrow,\downarrow\rangle + a(\downarrow,\downarrow,\uparrow;t)|\downarrow,\downarrow,\uparrow\rangle$$
$$+ \cdots + a(\uparrow,\uparrow,\uparrow;t)|\uparrow,\uparrow,\uparrow\rangle, \tag{2}$$

describes the state of the whole QC at time $t$. The complex coefficients $a(\downarrow,\downarrow,\downarrow;t),\ldots,a(\uparrow,\uparrow,\uparrow;t)$ completely specify the state of the quantum system. For the time-dependent Hamiltonian we take

$$H(t) = -J_{1,2,z}S_1^z S_2^z - J_{1,3,z}S_1^z S_3^z - J_{2,3,z}S_2^z S_3^z$$
$$- \sum_{j=1}^{3}\sum_{\alpha=x,y,z} h_{j,\alpha,0}S_j^\alpha$$
$$- \sum_{j=1}^{3}\sum_{\alpha=x,y} h_{j,\alpha,1}\sin(f_{j,\alpha}t + \phi_{j,\alpha})S_j^\alpha \tag{3}$$

where $S_j^\alpha$ denotes the $\alpha$th component of the spin-1/2 operator representing the $j$th qubit, $J_{j,k}$ determines the strength of the interaction between the qubits labelled $j$ and $k$, $h_{j,\alpha,0}$ and $h_{j,\alpha,1}$ represent the static (magnetic) and periodic (RF) field acting on the $j$th spin respectively. The frequency and phase of the periodic field are denoted by $f_{j,\alpha}$ and $\varphi_{j,\alpha}$. It is known that (3) is sufficiently general to serve as a model for a universal (three qubit) QC [7, 8]. The sinusoidal external fields in (3) will be used to simulate NMR pulses.

A QA for QC model (3) consists of a sequence of elementary operations that change the state $|\Psi\rangle$ of the quantum processor according to the TDSE, i.e. by (a product of) unitary transformations. We call these elementary operations micro instructions (MIs) in what follows. They are not exactly playing the same role as MIs do in digital processors, they merely represent the smallest units of operation of the quantum processor. The action of a MI on the state $|\Psi\rangle$ of the quantum processor is defined by specifying how long it acts (i.e. the time interval it is active), and the values of all the $J$ and $h$ appearing in (3). The $J$ and $h$ are fixed during the operation of the MI. A MI transforms the input state $|\Psi(t)\rangle$ into the output state $|\Psi(t+\tau)\rangle$ where $\tau$ denotes the time interval during which the MI is active. During this time interval the only time-dependence of $H(t)$ is through the sinusoidal modulation of the fields on the spins.

The QCE solves TDSE (1) by a Suzuki product-formula, i.e. in terms of elementary unitary operations [9–15]. For all practical purposes, the results obtained by this technique are indistinguishable from the exact solution of the TDSE.

### 2.2. Graphical user interface

A graphical user interface (GUI) has been developed to facilitate the specification of the MIs (to model the QC hardware) and the execution of the quantum programs (QPs). The QCE runs in a Windows 98/NT/2000 environment. Using the GUI requires no skills other than the basic ones needed to run a standard MS-Windows application. The QCE is freely distributed as a self-installing executable, containing the program, documentation, and various QPs[4].

The main window of the QCE (see figure 1 for example) contains a window showing the set of MIs that is currently

---

[4] http://rugth30.phys.rug.nl/compphys/qce.htm

24
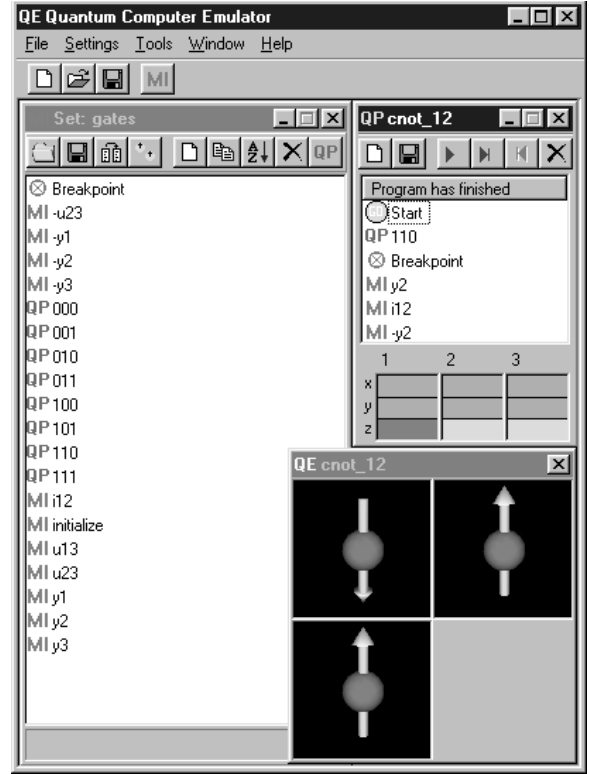


**Figure 1.** Picture of the QCE showing a window with a set of micro instructions implementing an ideal three qubit QC and a window with the quantum program for the CNOT gate operating on the $|110\rangle$ state. The final state of the QC, i.e. the expectation value of the qubits (spin operators), is shown at the bottom of the program window (dark grey = $|1\rangle$, light grey = $|0\rangle$). The QCE has an option to visualize the time evolution of the state of the QC in terms of arrows representing the expectation values of the qubits.

active and one or more windows containing the QPs. Tooltips appear when the mouse moves over the buttons, a standard Windows feature. Each MI set has two reserved MIs: 'breakpoint' to allow a QP to pause at a specified point and 'initialize' to specify the initial state of the QC (normally the first MI in a QP). The QCE supports the use of QPs as MIs (see figure 1). QPs can be added to a particular MI set through the button labelled 'QP' (top right of the MI set window). During execution, a QP that is called from another QP will call either another QP or a genuine MI from the currently loaded set of MIs. The QCE will skip all initialization MIs except for the first one. This facilitates the testing of QPs that are used as sub-QPs. A QP calling a MI or QP that cannot be found in the current MI set will generate an error message and stop.

Writing a QA on the QCE from scratch is a two-step process. First one has to specify the MIs, taking into account the particular physical realization of the QC that one wants to emulate. A new MI set is created by clicking on the 'MI' button at the top of the main window of the QCE. The MI set window offers all necessary tools to edit and manipulate the MIs. New MIs in the MI set window are obtained by clicking on the 'white page' button at the top of this window. The parameters specifying the MI can then be filled out. Existing MIs can be edited by double-clicking the MI icon.

The second step, writing a QP, consists of dragging and dropping MIs onto a 'QP' window. New 'QP' windows are created by clicking on the 'white page' button at the top of the main window of the QCE, old QPs are opened by clicking on the 'folder' button at the top of the main window of the QCE or by double-clicking on a QP in a 'MI set' window.

Execution of a QP on the QCE is realized by the control buttons at the top of the 'QP' program. The results of executing a QP appear in colour-coded form at the bottom of the corresponding 'QP' window. For each qubit the expectation value of the three spin components are shown: $Q_j^\alpha \equiv 1/2 - \langle S_j^\alpha \rangle$ ($\alpha = x, y, z$), green (light grey) corresponds to 0, red (dark grey) to 1. Usually one row of values (the $z$-component) will be of interest. Optionally the QCE visualizes the time evolution of the state of the QC in terms of arrows representing the expectation values of the qubits (see figure 1) and generates text files with the numerical results for further processing.

## 3. Elementary operations

One qubit or one spin-$1/2$ system is a two-state quantum system. The two basis states spanning the Hilbert space are denoted by $\langle \uparrow | \equiv (10) \equiv \langle 0|$ and $\langle \downarrow | \equiv (01) \equiv \langle 1|$. In quantum computation rotations of spin $j$ about $\pi/2$ around the $x$- and $y$-axis are frequently used operations. In matrix notation, they are given by

$$X_j \equiv e^{i\pi S_j^x/2} = \frac{1}{\sqrt{2}} \begin{pmatrix} 1 & i \\ i & 1 \end{pmatrix}, \qquad (4)$$

and

$$Y_j \equiv e^{i\pi S_j^y/2} = \frac{1}{\sqrt{2}} \begin{pmatrix} 1 & 1 \\ -1 & 1 \end{pmatrix}, \qquad (5)$$

respectively. With this notation we have for example

$$X_1 \begin{pmatrix} |00\rangle \\ |10\rangle \\ |01\rangle \\ |11\rangle \end{pmatrix} \equiv \frac{1}{\sqrt{2}} \begin{pmatrix} 1 & i & 0 & 0 \\ i & 1 & 0 & 0 \\ 0 & 0 & 1 & i \\ 0 & 0 & i & 1 \end{pmatrix} \begin{pmatrix} |00\rangle \\ |10\rangle \\ |01\rangle \\ |11\rangle \end{pmatrix}, \qquad (6)$$

where $|b_1 b_2\rangle \equiv |b_1\rangle |b_2\rangle$ and $b_i = 0, 1$. For example, $X_1|11\rangle = (|11\rangle + i|01\rangle)/\sqrt{2}$. Using the same labelling of states as in (6) we have

$$Y_2 \equiv \frac{1}{\sqrt{2}} \begin{pmatrix} 1 & 0 & 1 & 0 \\ 0 & 1 & 0 & 1 \\ -1 & 0 & 1 & 0 \\ 0 & -1 & 0 & 1 \end{pmatrix}, \qquad (7)$$

e.g. $Y_2|11\rangle = (|10\rangle + |11\rangle)/\sqrt{2}$. The matrix expressions for the inverse of the rotations $X_1$ and $Y_2$, denoted by $\overline{X}_1$ and $\overline{X}_2$ respectively, are obtained by taking the Hermitian conjugates of the matrices in (6) and (7). For example, $\overline{Y}_2|11\rangle = (|11\rangle - |10\rangle)/\sqrt{2}$.

$X_j$ and $Y_j$ represent operations on single qubits. Two qubits $j, k$ 'communicate' with each other through the interaction-controlled phase shift

$$I_{jk} \equiv \begin{pmatrix} e^{i\phi_{00}} & 0 & 0 & 0 \\ 0 & e^{i\phi_{10}} & 0 & 0 \\ 0 & 0 & e^{i\phi_{01}} & 0 \\ 0 & 0 & 0 & e^{i\phi_{11}} \end{pmatrix}. \qquad (8)$$

**Table 1.** Input (IN) and output (OUT) states for the CNOT gate.

| IN | OUT |
|------|------|
| $|00\rangle$ | $|00\rangle$ |
| $|10\rangle$ | $|11\rangle$ |
| $|01\rangle$ | $|01\rangle$ |
| $|11\rangle$ | $|10\rangle$ |

## 4. CNOT gate

The CNOT gate flips the second qubit if the first qubit is down, i.e. the first qubit acts as a control qubit for the second one, see table 1.

Assume that the QC is in a state

$$|\Psi\rangle = a_0|00\rangle + a_1|10\rangle + a_2|01\rangle + a_3|11\rangle. \qquad (9)$$

First we apply to $|\Psi\rangle$ the rotation operator $Y_2$, as defined in (7). This results in

$$Y_2|\Psi\rangle = [(a_0 + a_2)|00\rangle + (a_1 + a_3)|10\rangle + (a_2 - a_0)|01\rangle \\ + (a_3 - a_1)|11\rangle]/\sqrt{2}. \qquad (10)$$

Next we apply to $Y_2|\Psi\rangle$ the interaction-controlled phase shift $I_{12}$

$$I_{12} Y_2|\Psi\rangle = \frac{1}{\sqrt{2}} \left\{ e^{i\phi_{00}} c_0|00\rangle + e^{i\phi_{10}} c_1|10\rangle \\ + e^{i\phi_{01}} c_2|01\rangle + e^{i\phi_{11}} c_3|11\rangle \right\} : \qquad (11)$$

where $c_0 = a_0 + a_2$, $c_1 = a_1 + a_3$, $c_2 = a_2 - a_0$ and $c_3 = a_3 - a_1$. Finally, we apply the inverse of the rotation $Y_2$

$$\overline{Y}_2 I_{12} Y_2|\Psi\rangle = \frac{1}{2} \left\{ [e^{i\phi_{00}} c_0 - e^{i\phi_{01}} c_2]|00\rangle \\ + [e^{i\phi_{10}} c_1 - e^{i\phi_{11}} c_3]|10\rangle + [e^{i\phi_{00}} c_0 + e^{i\phi_{01}} c_2]|01\rangle \\ + [e^{i\phi_{10}} c_1 + e^{i\phi_{11}} c_3]|11\rangle \right\}. \qquad (12)$$

Since the CNOT gate will not change $a_0$ and $a_2$ (see table 1) we can choose $\phi_{00} = \phi_{01}$. Then (12) results in

$$\overline{Y}_2 I_{12} Y_2|\Psi\rangle = e^{i\phi_{00}} \left\{ a_0|00\rangle + a_2|01\rangle \\ + e^{i\beta} (a_1 \cos\alpha + i a_3 \sin\alpha)|10\rangle \\ + e^{i\beta} (a_3 \cos\alpha + i a_1 \sin\alpha)|11\rangle \right\} \qquad (13)$$

where $\beta = \alpha + \phi_{11} - \phi_{00}$ and $\alpha = (\phi_{10} - \phi_{11})/2$. The global phase factor $e^{i\phi_{00}}$ is physically irrelevant.

We can implement the interaction-controlled phase shift, i.e. $I_{12} = e^{-i\tau H}$, by means of the most simple spin-$1/2$ system, i.e. the Ising model

$$H = -J S_1^z S_2^z - h(S_1^z + S_2^z). \qquad (14)$$

Then the values for $\phi_{mn}$ are $\phi_{00} = \tau(J/4 + h)$, $\phi_{10} = \phi_{01} = -\tau J/4$ and $\phi_{11} = \tau(J/4 - h)$. With these values for $\phi_{mn}$ and taking into account our choice $\phi_{00} = \phi_{01}$, (13) results in

$$\overline{Y}_2 I_{12} Y_2|\Psi\rangle = e^{i\alpha/2} \left\{ a_0|00\rangle + a_2|01\rangle \\ + e^{-i\alpha} (a_1 \cos\alpha + i a_3 \sin\alpha)|10\rangle \\ + e^{-i\alpha} (a_3 \cos\alpha + i a_1 \sin\alpha)|11\rangle \right\}. \qquad (15)$$

Using the same labelling of states as in (6) we have

$$\overline{Y}_2 I_{12} Y_2 = \begin{pmatrix} 1 & 0 & 0 & 0 \\ 0 & e^{-i\alpha}\cos\alpha & 0 & ie^{-i\alpha}\sin\alpha \\ 0 & 0 & 1 & 0 \\ 0 & ie^{-i\alpha}\sin\alpha & 0 & e^{i\alpha}\cos\alpha \end{pmatrix} \qquad (16)$$

where we dropped the global phase factor $e^{i\alpha/2}$. If we choose $\alpha = \pi/2$ operating with the operator $\overline{Y}_2 I_{12} Y_2$ on the states $|00\rangle$, $|10\rangle$, $|01\rangle$ and $|11\rangle$ results in $|00\rangle$, $|11\rangle$, $|01\rangle$ and $|10\rangle$. Hence the CNOT gate can be implemented by $\overline{Y}_2 I Y_2$ where $\alpha = \pi/2$ and $\phi_{00} = \phi_{01} = \phi_{10} = \alpha/2$, $\phi_{11} = -3\alpha/2$.

The example of the CNOT gate provided in the QCE software distribution uses three instead of two qubits because three qubits are required for implementation of the Toffoli gate (see next section). The same QC and elementary operations can then be used for both the CNOT and the Toffoli gate. To illustrate the functionality of the QCE we describe the main steps of how to program a three qubit QC so that it gives the outcome of a CNOT gate operating on the $|110\rangle$ state. The details can be found in the MI set 'gates' and the QP 'cnot_12' (see figure 1), which we built for this purpose and are included in the QCE distribution.

First the QC has to be initialized (setting each of the three qubits to $|0\rangle$) and then the first and second qubit have to be put in the state $|1\rangle$. On the QCE this is accomplished by the QP 'QP110' which consists of the sub-QPs 'QP 000', 'QP 100' and 'QP 010'. 'QP000' only contains the MI 'initialize', a reserved MI in the QCE (see above), and puts the QC in the state $|000\rangle$. 'QP 100' ('QP010') consists of two MIs '$Y_1$' ('$Y_2$') and rotates clockwise qubit 1 (qubit 2) about $\pi$ around the $y$-axis. One single MI '$Y_1$' rotates clockwise qubit 1 about $\pi/2$ around the $y$-axis. This is done by choosing the parameters in the MI '$Y_1$' such that $-i\tau H = i\pi S_j^y/2$, where $H$ is given by (3) with $h_{j,\alpha,1} = 0$. In practice this means taking $h_{1,y,0} = 1$, $\tau/2\pi = 1/4$ and all other parameters zero. 'QP 110' puts the QC in the state $|110\rangle$, the starting position for our particular example.

The next task is to implement the CNOT gate itself. First we rotate clockwise qubit 2 about $\pi/2$ around the $y$-axis by means of the MI '$Y_2$'. This brings the QC in the state $(|100\rangle + |110\rangle)/\sqrt{2}$. Then we apply the interaction-controlled phase shift $I_{12}$. We construct the MI '$I_{12}$' by taking the parameters such that $-i\tau H = i\phi_{11}$, i.e. $J_{1,2,z} = -1$, $h_{1,z,0} = h_{2,z,0} = 1/2$, $\tau/2\pi = 1/2$ and all other parameters zero. Apart from some global phase factor this brings the QC in the state $(|100\rangle - |110\rangle)/\sqrt{2}$. Finally, operating with $\overline{Y}_2$ on this state results in $|100\rangle$ as the end state of the QC. The expectation values of the three qubit components are $Q_1^x = Q_1^y = 0.5$, $Q_1^z = 1$ and $Q_2^x = Q_3^x = Q_2^y = Q_3^y = 0.5$, $Q_2^z = Q_3^z = 0$.

## 5. Toffoli gate

The Toffoli gate works with two control qubits: only if the first two qubits ($Q_1$, $Q_2$) are down is the third qubit ($Q_3$) flipped (see table 2). A schematic representation of the Toffoli gate is given in figure 2 [16]. A dot and a cross connected by a vertical line represent a CNOT gate: if the qubit on the horizontal line with a dot equals one, the qubit on the horizontal line with a cross flips. A similar rule applies to the qubits connected by a vertical line with as endpoints a dot and a box with an operator $V$ or $\overline{V}$. Only if the qubit corresponding to the dot equals one is operation $V$ or $\overline{V}$ carried out.
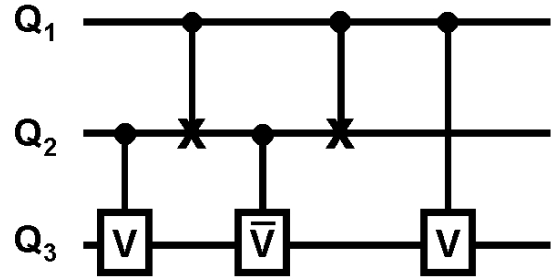
The operation of the Toffoli gate is demonstrated in table 3. The first two columns give all possible combinations of qubits $Q_1$ and $Q_2$. The next five columns show schematically the outcome of the various operations that build up the Toffoli gate

**Table 2.** Input (IN) and output (OUT) states for the Toffoli gate.

| IN | OUT |
|---|---|
| $|000\rangle$ | $|000\rangle$ |
| $|100\rangle$ | $|100\rangle$ |
| $|010\rangle$ | $|010\rangle$ |
| $|001\rangle$ | $|001\rangle$ |
| $|110\rangle$ | $|111\rangle$ |
| $|101\rangle$ | $|101\rangle$ |
| $|011\rangle$ | $|011\rangle$ |
| $|111\rangle$ | $|110\rangle$ |

**Table 3.** Operation of the Toffoli gate.

| $Q_1$ | $Q_2$ | ‖ | $V$ | CNOT | $\overline{V}$ | CNOT | $V$ | ‖ | $Q_3$ |
|---|---|---|---|---|---|---|---|---|---|
| 0 | 0 | ‖ | x | x | x | x | x | ‖ | $Q_3$ |
| 1 | 0 | ‖ | x | 1 | $\overline{V}$ | 0 | $V$ | ‖ | $\overline{V}V Q_3$ |
| 0 | 1 | ‖ | $V$ | x | $\overline{V}$ | x | x | ‖ | $V\overline{V}Q_3$ |
| 1 | 1 | ‖ | $V$ | 0 | x | 1 | $V$ | ‖ | $V^2 Q_3$ |



**Figure 2.** Schematic representation of the Toffoli gate.

(see figure 2). In the columns labelled 'CNOT' only the value of qubit $Q_2$ is shown since $Q_1$ acts as a control bit and does not change. A cross means that the operation is not carried out because the control bit is zero. The last column shows the final operation on the third qubit. From tables 2 and 3 it follows that operation $V$ has to be constructed such that $V^2$ flips $Q_3$ and that $\overline{V} V$ is equal to the identity matrix. These conditions are fulfilled by taking

$$V = \frac{e^{-i\pi/4}}{\sqrt{2}} \begin{pmatrix} 1 & i \\ i & 1 \end{pmatrix}. \tag{17}$$

For example, $V_{12}$ can be written as $\overline{Y}_2 U_{12} Y_2$ where $V_{12}$ is given by the matrix in (16) with $\alpha$ replaced by $\pi/4$. Hence the Toffoli gate can be implemented by the following sequence of operations:

$$\overline{Y}_3 U_{13} Y_3 \overline{Y}_2 I_{12} Y_2 \overline{Y}_3 \overline{U}_{23} Y_3 \overline{Y}_2 I_{12} Y_2 \overline{Y}_3 U_{23} Y_3. \tag{18}$$

This sequence can be shortened by observing that in some cases a rotation is followed by its inverse. This leads to

$$\overline{Y}_3 U_{13} \overline{Y}_2 I_{12} Y_2 \overline{U}_{23} \overline{Y}_2 I_{12} Y_2 U_{23} Y_3. \tag{19}$$

The implementation of the Toffoli gate on the QCE is very similar to the implementation of the CNOT gate. Therefore, we only mention here the two QPs that are delivered with the QCE. QP 'toffoli' implements the toffoli gate by means of (18) and QP 'toffoli-optimized' by means of the sequence (19).

## 6. CNOT gate on a NMR quantum computer

Sections 4 and 5 described the implementation of the CNOT and the Toffoli gate on an ideal QC. Our aim in this section is to illustrate how to implement the CNOT gate on a two qubit NMR-like QC and how to simulate this with the QCE.

In the NMR experiments [5, 6] the two nuclear spins of the ($^1$H and $^{13}$C atoms in a carbon-13 labelled chloroform) molecule are placed in a strong magnetic field in the $+z$-direction. In the absence of interactions with other degrees of freedom this spin-1/2 system can be modelled by the Hamiltonian

$$H^{\text{NMR}} = -J_{1,2,z} S_1^z S_2^z - h_{1,z,0} S_1^z - h_{2,z,0} S_2^z \qquad (20)$$

where $h_{1,z,0}/2\pi \approx 500$ MHz, $h_{2,z,0}/2\pi \approx 125$ MHz, and $J_{1,2,z}/2\pi \approx -215$ Hz [5].

NMR uses radiofrequency electromagnetic pulses to rotate the spins. By tuning the frequency of the RF-field to the precession frequency of a particular spin, the power of the applied pulse (= intensity times duration) controls how much the spin will rotate. The axis of the rotation is determined by the direction of the applied RF-field.

The elementary model of a NMR experiment of a single spin (qubit 1 for example) subject to a constant magnetic field along the $z$-axis and a RF-field along the $x$-axis reads [17]

$$i\frac{\partial}{\partial t}|\Phi(t)\rangle = -\big[h_{1,z,0} S_1^z + h_{1,x,1} S_1^x \sin f_{1,x}t\big]|\Phi(t)\rangle, \quad (21)$$

where $|\Phi(t=0)\rangle$ is the initial state of the two-state system and we have set the phase $\varphi_{1,x} = 0$ in (21). Substituting $|\Phi(t)\rangle = e^{itf S_1^z}|\Psi(t)\rangle$ and choosing $f = h_{1,z,0}$ yields

$$i\frac{\partial}{\partial t}|\Psi(t)\rangle = -h_{1,x,1}\big[S_1^x \sin f_{1,x}t \cos ft$$
$$+ S_1^y \sin f_{1,x}t \sin h_{1,z,0}t\big]|\Psi(t)\rangle. \qquad (22)$$

At resonance, i.e. $f_{1,x} = h_{1,z,0}$, we find

$$i\frac{\partial}{\partial t}|\Psi(t)\rangle = -\frac{h_{1,x,1}}{2}\big[S_1^y + S_1^x \sin 2h_{1,z,0}t$$
$$- S_1^y \cos 2h_{1,z,0}t\big]|\Psi(t)\rangle. \qquad (23)$$

Assuming that the effects of the higher harmonic terms (i.e. the terms in $\sin 2h_{1,z,0}t$ and $\cos 2h_{1,z,0}t$) are small [17], (23) is easily solved to give

$$|\Psi(t)\rangle \approx e^{ith_{1,x,1}S_1^y/2}|\Psi(t=0)\rangle, \qquad (24)$$

so that the overall action of a RF-pulse of duration $\tau$ can be written as

$$|\Phi(t+\tau)\rangle \approx e^{i\tau h_{1,z,0}S_1^z} e^{i\tau h_{1,x,1}S_1^y/2}|\Phi(t)\rangle. \qquad (25)$$

Hence it follows that application of an RF-pulse of 'power' $\tau h_{1,x,1} = \pi$ will have the effect of rotating the spin by an angle of $\pi/2$ about the $y$-axis.

For the implementation of the CNOT gate it is expedient to write Hamiltonian (20) as $H^{\text{NMR}} = H + H'$, where $H$ is given by (14) and $H' = (h - h_{1,z,0})S_1^z + (h - h_{2,z,0})S_2^z$. The CNOT gate can then be implemented by

$$\overline{Y}_2 I_{12} Y_2 = e^{-i\tau(h_{1,z,0}-h)S_1^z} e^{-i\tau(h_{2,z,0}-h)S_2^z} \overline{Y}_2 e^{-i\tau H^{\text{NMR}}} Y_2. \qquad (26)$$

Guided by the experiments [5, 6], we take, for the implementation of this CNOT gate on the QCE, the parameters $h_{1,z,0} = 1$, $h_{2,z,0} = 1/4$ and $J_{1,2,z} = -10^{-6}$. In all operations these values are fixed since they are determined by the molecules used in the NMR experiment. As usual, we initialize the QC by means of MI 'initialize' (using the parameters mentioned above). Then, as an example, we put the two qubits in state $|1\rangle$ by means of MI '$Y_1$' and MI '$Y_2$'. The parameters in the MI '$Y_2$' for example, are chosen as follows: rotating spin 2 about the $y$-axis in an NMR experiment leads to $f_{2,x} = h_{2,z,0} = f_{1,x} = 1/4$. Rotation by an angle of $\pi/2$ requires $\tau h_{2,x,1} = \pi$. Choosing $h_{2,x,1} = 1/80$ gives $h_{1,x,1} = 0.05$ and $\tau/2\pi = 40$. All other parameters, except for $h_{1,z,0}$, $h_{2,z,0}$ and $J_{1,2,z}$, are zero. For the MI '$Y_1$' we choose $f_{1,x} = h_{1,z,0} = f_{2,x} = 1$, $h_{1,x,1} = 1/40$, $h_{2,x,1} = 1/160$ and $\tau/2\pi = 20$.

Implementation of the CNOT gate itself requires $(\tau/2\pi)J = -1/2$ and $(\tau/2\pi)h = 1/4$ (see section 4). Hence, $\tau/2\pi = 0.5 \times 10^6$ and $h = 0.5 \times 10^{-6}$. Using this condition and the fact that $\tau h_{1,z,0}/2\pi = 500\,000$ and $\tau h_{2,z,0}/2\pi = 125\,000$, (26) can be written as

$$\overline{Y}_2 I_{12} Y_2 = e^{i\pi S_1^z/2} e^{i\pi S_2^x/2} \overline{Y}_2 e^{-i\tau H^{\text{NMR}}} Y_2$$
$$= \overline{X}_1 Y_1 X_1 X_2 \overline{Y}_2 I_{12} I_2. \qquad (27)$$

For MI '$X_2$' we choose $f_{2,y} = h_{2,z,0} = f_{1,y} = 1/4$, $h_{2,y,1} = -1/80$, $h_{1,y,1} = -0.05$ and $\tau/2\pi = 40$ and for MI '$X_1$': $f_{1,y} = h_{1,z,0} = f_{2,y} = 1$, $h_{1,y,1} = -1/40$, $h_{2,y,1} = -1/160$ and $\tau/2\pi = 20$. For MI '$I_{12}$' we take the parameter values $J_{1,2,z} = -10^{-6}$, $h_{1,z,0} = 1$, $h_{2,z,0} = 1/4$, $\tau/2\pi = 500\,000$, and all others zero. As a result of the application of sequence (27) on the state $|11\rangle$ the final state of the QC becomes $|10\rangle$, as required. However, the expectation values of the three components of the qubits slightly differ from the ones obtained on the ideal QC (see section 4): $Q_1^x = 0.510$, $Q_1^y = 0.489$, $Q_1^z = 1$ and $Q_2^x = 0.519$, $Q_2^y = 0.5$, $Q_2^z = 0$. This is due to the approximate nature of the operations used in the NMR case.

## 7. Summary

We have demonstrated the use of the QCE as an educational tool to learn interactively about QCs and quantum algorithms. For pedagogical reasons the use of the QCE has been illustrated through the implementation of the CNOT and Toffoli gate on QCs using ideal and more realistic units, such as those of NMR-like QCs. Additional examples, including several popular quantum algorithms, can be found in [9, 15] and in the QCE software distribution itself.

## Acknowledgments

## References

[1] Shor P 1994 *Proc. 35th Annu. Symp. on Foundations of Computer Science* ed S Goldwasser (Los Alamitos, CA: IEEE Computer Society Press) p 124
[2] Grover L K 1997 *Phys. Rev. Lett.* **79** 4709
[3] Jones J A and Mosca M 1998 *J. Chem. Phys.* **109** 1648

[4] Jones J A, Mosca M and Hansen R H 1998 *Nature* **393** 344
[5] Chuang I L, Vandersypen L M K, Xinlan Zhou, Leung D W and Lloyd S 1998 *Nature* **393** 143
[6] Chuang I L, Gershenfeld N and Kubinec M 1998 *Phys. Rev. Lett.* **80** 3408
[7] Lloyd S 1993 *Science* **261** 1569
[8] Berman G P, Doolen G D, Holm D D and Tsifrinovich V I 1994 *Phys. Lett.* A **193** 444
[9] De Raedt H, Hams A H, Michielsen K and De Raedt K 2000 *Comput. Phys. Commun.* **132** 1
[10] Suzuki M, Miyashita S and Kuroda A 1977 *Prog. Theor. Phys.* **58** 1377
[11] De Raedt H 1987 *Comput. Phys. Rep.* **7** 1
[12] Suzuki M 1993 *Proc. Japan Acad.* B **69** 161
[13] de Vries P and De Raedt H 1993 *Phys. Rev.* B **47** 7929
[14] De Raedt H and Michielsen K 1994 *Comput. Phys.* **8** 600
[15] De Raedt H, Hams A, Michielsen K, Miyashita S and Saito K 2000 *J. Phys. Soc. Japan* **69** 401
[16] Barenco A, Bennett C H, Cleve R, DiVincenzo D P, Margolus N, Shor P, Sleator T, Smolin J A and Weinfurter H 1995 *Phys. Rev.* A **52** 3457
[17] Baym G 1974 *Lectures on Quantum Mechanics* (Reading, MA: Benjamin)